THE UNIVERSITY OF RHODE ISLAND

University of Rhode Island
DigitalCommons@URI

Chemistry Faculty Publications

Chemistry

1989

Monte Carlo Studies of Hydrogen Flouride Clusters: Cluster Size Distributions in Hydrogen Flouride Vapor

Changyin Zhang
University of Rhode Island

David L. Freeman
University of Rhode Island, dfreeman@uri.edu

Jimmie D. Doll

Follow this and additional works at: https://digitalcommons.uri.edu/chm_facpubs

Terms of Use
All rights reserved under copyright.

Citation/Publisher Attribution
Zhang, C., Freeman, D. L., & Doll, J. D. (1989). Monte Carlo Studies of Hydrogen Fluoride Clusters: Cluster Size Distributions in Hydrogen Fluoride Vapor. *J. Chem. Phys. 91*(4), 2489 (1989). doi: 10.1063/1.457008
Available at: http://dx.doi.org/10.1063/1.457008

This Article is brought to you for free and open access by the Chemistry at DigitalCommons@URI. It has been accepted for inclusion in Chemistry Faculty Publications by an authorized administrator of DigitalCommons@URI. For more information, please contact digitalcommons-group@uri.edu.

Monte Carlo Studies of Hydrogen Flouride Clusters: Cluster Size Distributions in Hydrogen Flouride Vapor

Publisher Statement
© 1989 American Institute of Physics.

Terms of Use
All rights reserved under copyright.

This article is available at DigitalCommons@URI: https://digitalcommons.uri.edu/chm_facpubs/32

Monte Carlo studies of hydrogen fluoride clusters: Cluster size distributions in hydrogen fluoride vapor

Changyin Zhang[a] and David L. Freeman
Department of Chemistry, The University of Rhode Island, Kingston, Rhode Island 02881-0801
J. D. Doll[b]
Chemistry Division, Los Alamos National Laboratory, MS G738, Los Alamos, New Mexico 87545

(Received 14 March 1989; accepted 25 April 1989)

An investigation into the structure and composition of hydrogen fluoride vapor is reported. Calculations are performed using a modified central force model potential developed by Klein and McDonald. Using a simulated annealing procedure, minimum energy structures for HF clusters are investigated ranging in size from $n = 2$ to 7. Good agreement is found for the structural parameters obtained from the model potential and other theoretical and experimental information. The Monte Carlo method is used to determine the thermodynamic energy, entropy, and Gibbs free energy of the hydrogen fluoride clusters at 1 atm pressure and 100 and 273 K. A minimum in the Gibbs free energy change is found at $n = 4$ implying that tetramers are very important in the vapor.

I. INTRODUCTION

The great importance of hydrogen bonding to physical and biological processes has led to considerable experimental and theoretical interest in hydrogen bonded systems over many years. One of the most widely studied hydrogen bonded materials is hydrogen fluoride in the gas, liquid, and solid phases. The particular interest in HF is a consequence of its small size and the strength of the hydrogen bonds that it forms. Experimental efforts have included infrared and microwave spectroscopy in the gas[1–8] and liquid[9,10] phases, and electron diffraction experiments in the gas phase.[11] There are a number of intriguing structural questions which have arisen from the experimental efforts. In the gas phase, HF is believed to consist primarily of ring-like clusters. It has been inferred that the dominant species in the gas phase within 50 deg of the boiling point may be either dimer, tetramer,[9,10] or hexamer.[11,12] The relative populations of these species is unknown, and the mechanism which would favor one species over another is also uncertain. In the condensed phases, HF is known to form long chains.[12] The mechanism that induces the transition between the ring-like structures expected for small HF clusters and the chains known to occur in the solid state is of considerable interest.

To understand the structure of HF more fully in its condensed phases, there has been considerable theoretical effort in providing descriptions of the system. Much of the work has focused on *ab initio* investigations of small HF clusters and the parallel development of approximate empirical potentials useful in the description of the system. One of the earliest *ab initio* studies was by Del Bene and Pople[13] who investigated HF clusters of size 3 to 6 using a minimum basis at the Hartree–Fock level. From the calculations, Del Bene and Pople concluded that all clusters of size three and above should be cyclic and the gas phase could be expected to be a mixture of monomers through hexamers. They also found the hexamer structures to be planar. Additional *ab initio* studies on the dimer, trimer, and tetramer were performed by Gaw *et al.*,[14] Scuseria and Schaefer,[15] Karpfen *et al.*,[16] Liu *et al.*,[17] and Latajka and Scheiner.[18] Good agreement was obtained between the *ab initio* results and the known experimental structure of the dimer.[5] The trimer, whose experimental structure only has been inferred quite recently,[8] is now agreed to have a cyclic planar structure. The computational work on the trimer seems to indicate that the cluster has no local minima in the potential surface other than the cyclic structure.[17] Of course, verifying that potential minima do not exist is quite difficult, and we will discuss this finding later in this paper.

From a combination of theoretical computations and experimental parameters, a number of model potential functions have been developed to describe the interactions between two HF monomers.[19–23] These potentials have been used in quantum scattering calculations and in numerical simulation studies of liquid HF.[20,21,24] In the liquid state calculations it has been assumed that the many-body potential can be represented as a pairwise sum over the HF dimer potentials. Although the assumption of two-body additivity has been critiqued,[13] the agreement between computed properties and experiment has been reasonable. Structurally, HF liquid was found to consist of long intertwined chains.[24] There was no evidence of the formation of rings in the simulations.

In the current work, we present results of Monte Carlo calculations of the thermodynamic properties and structure of HF clusters ranging in size from $n = 2$ to 7. Our particular interest is in the composition of HF vapor. Consequently, our primary focus has been in the calculation of the Gibbs free energies of the clusters. Our interest in this system has been somewhat motivated by previous work on argon clusters.[25,26] In studies of the Gibbs free energy of argon clusters, it was found that certain clusters sizes were particularly stable. The extra stability of such cluster sizes in argon were related to the magic numbers observed in cluster beams.[27] It seems natural to identify the analog of the magic number

[a] Present address: IPI Imaging Products, 666 Third Ave, c/o Profile Diagnostics, New York, NY 10017.
[b] Present address: Department of Chemistry, Brown University, Providence, RI 02912.

 0021-9606/89/162489-09$02.10 © 1989 American Institute of Physics

structure observed for weakly bound clusters like argon, with extra stable clusters that should be observable for strongly bound complexes like HF in the vapor phase. Consequently we expect that we can identify the most important species in HF vapor by their Gibbs free energy minima. Correlation of magic number behavior in the Gibbs free energy with zero temperature structures was quite successful in the case of argon,[26] and a comparison of structure with stability will be made in the case of HF.

The contents of the remainder of this paper are as follows. In Sec. II we discuss the model potential used in this work. Since the potential surface we have chosen is one of the simplest available, we also consider our criteria for assessing the quality of the potential function. Our principal test is the structures predicted by the model potential. We identify these potential minima by a Brownian simulated annealing procedure, which we outline in Sec. III. In Sec. III, we also present the results of our annealing studies. In Sec. IV we examine the method used to calculate the Gibbs free energies of the clusters. In Sec. V we present our results, and a discussion of their significance is given in Sec. VI.

II. THE MODEL POTENTIAL

A number of model potentials have been developed for the interaction of two HF molecules.[19–23] The most sophisticated of these potentials[22,23] have been used primarily in quantum scattering calculations. For the most part, the potentials used in numerical simulation studies of condensed phases[19–21] have been significantly simpler. One of the simplest is a strict central force model (named HF2) adopted by Klein and McDonald[21] from a potential developed by Stillinger.[28] When used by Klein and McDonald,[21] the intramolecular degrees of freedom were suppressed so that each monomer unit in the dimer was kept rigid. The HF2 potential was found to have at least two minima; one in a linear structure and another of lower energy in the experimentally known bent structure.[5] We have verified the Klein–McDonald model predicts these two potential minima. As we shall show in Sec. III, when the restriction of rigid monomer bond lengths is removed from the HF2 potential, only the bent structure is a minimum of the potential surface. Indeed, as we shall see, the molecular structural parameters are in good agreement with *ab initio* calculations and experimental information. For future reference, we display the potential we used in the calculations here. The units of energy are kcal mol^{-1} and the units of length are angstroms. The potential function for the intermolecular interactions is given by

$$V_{FF}(r) = (3\times 10^4)/r^9 - \exp[-4(r-2.9)^2] + 56.72/r, \tag{1a}$$

$$V_{HH}(r) = 20/\{1+\exp[20(r-1.95)]\} - 21.7\exp[-4.5(r-1.412)^2] + 0.7\exp[-12(r-2.7)^2] + 56.72/r, \tag{1b}$$

$$V_{FH}(r) = 3.87/r^8 - 0.7\exp[-10(r-3)^2] - 5/\{1+\exp[5(r-2)]\} - 56.72/r, \tag{1c}$$

where V_{FF}, V_{HH}, and V_{FH} represent interactions between two fluorine atoms, two hydrogen atoms, and a fluorine and a hydrogen atom, respectively. For the interactions of hydrogen and fluorine atoms on the same molecule we use a Morse potential

$$\tilde{V}_{HF}(r) = 141.4\{1-\exp[-2.256(r-0.917)]\}^2. \tag{2}$$

The parameters in Eq. (2) were obtained by a fit to spectroscopic data.[28]

As is well known, the definition of a cluster in a vapor is ambiguous. This ambiguity has led to a number of useful approaches to assigning molecules to a particular cluster.[30,31] In previous Monte Carlo calculations of the free energy of clusters of argon[25,26,31] and water,[32,33] the clusters were defined with reference to a constraining potential. Although the work reported here is strictly classical, we are currently extending the calculations to include quantum effects using Fourier path integral methods.[34] As in previous work on argon, path integral calculations are facilitated by applying a continuous constraining potential. Consequently we define our clusters by confining each monomer unit with the continuous constraining potential

$$V_c(\mathbf{r}_H,\mathbf{r}_F) = [(\mathbf{R}_{HF} - \mathbf{R}_{c.m.})/R_c]^{20}, \tag{3}$$

where $\mathbf{r}_H$ and $\mathbf{r}_F$ are the coordinates of the hydrogen and the fluorine atoms respectively, $\mathbf{R}_{HF}$ is the coordinate of the center of mass of the HF monomer,

$$\mathbf{R}_{HF} = (m_H\mathbf{r}_H + m_F\mathbf{r}_F)/(m_H + m_F), \tag{4}$$

$\mathbf{R}_{c.m.}$ is the coordinate of the center of mass of the cluster,

$$\mathbf{R}_{c.m.} = (1/M)\sum_i^N m_i\mathbf{r}_i, \tag{5}$$

and R_c is a constraining radius to be specified later. In Eq. (5), M is the total mass of the cluster containing N atoms. This same form for the constraining potential was used in the path integral Monte Carlo calculations on argon clusters by Freeman and Doll.[25,26] In the case of argon, the calculated free energies were found to be insensitive to the chosen constraining radius.[31] We shall verify that the same insensitivity applies in the case of HF later in this paper.

III. SIMULATED ANNEALING STUDIES

As we indicated in Sec. II, Klein and McDonald[21] found that the HF2 potential predicted at least two minima for the HF dimer when the intramolecular motions were excluded. As we shall show shortly, when the coordinates of the hydrogen and fluorine atoms within a monomer are allowed to relax, only one structure for the dimer is found, and it agrees well with experiment and theoretical *ab initio* calculations. In general, we have tested the quality of the potential by locating the minimum energy structures for the clusters studied. We have found the HF2 potential to give a structure for the trimer which also agrees well with experiment and *ab initio* calculations. The structures of clusters larger than $n = 3$ have not been explored in any detail elsewhere.

As in any many-body system, the larger clusters can be expected to have many local potential minima, and the number of such minima can be expected to grow exponentially with cluster size.[35] A method of locating potential minima

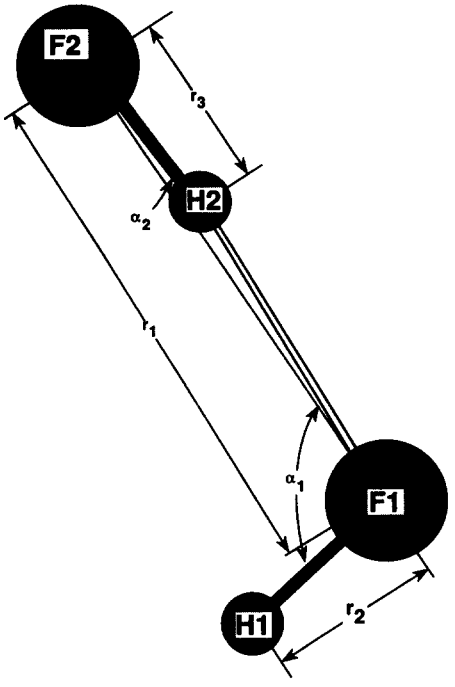

FIG. 1. The structure for $(HF)_2$ obtained from the HF2 potential. The labels for the angles and bond lengths are in accord with the data in Table I. The dark lines represent covalent bonds between H and F atoms on the same molecule and the light double lines represent the hydrogen bonds.

which has proved useful at least for small clusters is simulated annealing. The simulated annealing method used here is similar to the Brownian quench approach used by Biswas and Hamann[36] for silicon clusters and identical to that used by Freeman, Doll, and Amar[37] for argon clusters. In this approach, for a cluster of size n, we place n HF monomers with random coordinates within a hard wall constraining potential and the system is "placed" in a Brownian heat bath. For the simulated annealing studies, the temperature of the bath was arbitrarily set to 300 K. The coordinates of the atoms in the cluster were then propagated by solution of the Langevin equation

$$\frac{d\mathbf{v}_i}{dt} = -\gamma \mathbf{v}_i + (1/m_i)\mathbf{F}_1 + (1/m_i)\mathbf{F}_2(t) , \qquad (6)$$

where $\mathbf{v}_i(t)$ is the velocity of particle i with mass m_i at time t, γ is a friction constant, $\mathbf{F}_1$ is the force on particle i due to the other atoms in the system as well as the constraining potential [Eqs. (1)–(3)] and $\mathbf{F}_2(t)$ is a random force having the property that

$$\langle \mathbf{F}_2(t)\mathbf{F}_2(t') \rangle = 2\gamma m_i^2 kT\delta(t-t') . \qquad (7)$$

Equation (6) was solved by methods implicit in Eq. (240) of the classic review of Brownian dynamics by Chandrasekhar[38] using Gaussian random noise for the integrated random force. After a warmup period the temperature of the system was set instantaneously to zero, and the cluster was allowed to relax to a potential minimum. With the exception of the dimer, multiple minima were found for all clusters studied. While we cannot prove that all local minima are found in this fashion, by performing on the order of 1000 annealing trajectories for each cluster size, we can be reasonably sure that we have found the lowest energy isomer as well as most of the important isomers.

In the case of the dimer, only one potential minimum was found. The structure, displayed in Fig. 1, has the same qualitative features to the known experimental[5] structure and the structures obtained from a number of *ab initio* calculations.[16,17] In Table I, we compare the calculated parameters for the dimer structure obtained from the HF2 potential with previous experimental and theoretical work. The definitions of the parameters shown in Table I are given in Fig. 1. The agreement between the predictions of the HF2 potential and structural parameters found by others is excellent.

The trimer was found to have five local minima in the HF2 potential. The lowest energy structure is the planar ring shown in Fig. 2. This planar structure is in good qualitative agreement with the known experimental[8] and theoretical[16,17] structure of the cluster. The parameters for the trimer are defined in Fig. 2, and a comparison of the parameters with previous work is given in Table II. The agreement between the calculations is quite good, although there is more uncertainty in the known structure of the trimer than the dimer. The probable cause of the stability of the trimer relative to an open chain structure is the extra hydrogen bond that is formed.

The additional local minima for the trimer have not been found in previous calculations. The structure next lowest in energy to the planar triangle is shown in Fig. 3. As can be seen, it is an open chain of *cis* geometry. A natural question is the energy barrier to deformation of the local minimum to the planar lowest energy structure. We have explored this energy barrier by using the modification of the

TABLE I. Structural parameters for the HF dimer.

	r_1[a]	r_2[a]	r_3[a]	α_1	α_2
Liu *et al.*[b]	2.804	0.903	0.910	121°	7°
Karpfen *et al.*[c]	2.83			123°	6°
Howard *et al.*[d] (experimental)	2.72 ± 0.03			$117° \pm 6°$	$10° \pm 6°$
Present	2.702	0.918	0.930	115°	10°

[a] Distances in angstroms.
[b] Reference 17.
[c] Reference 16.
[d] Reference 5.

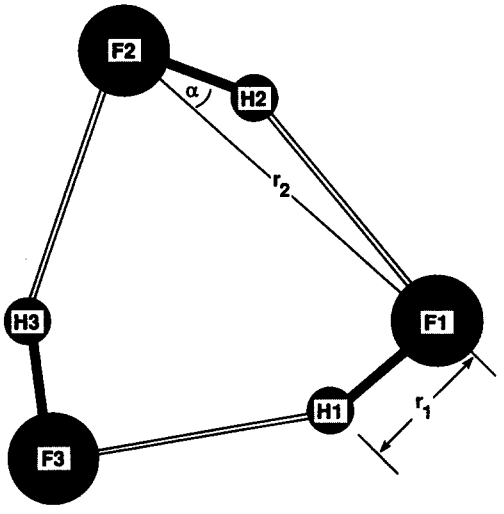

FIG. 2. The cyclic structure for $(HF)_3$ obtained from the HF2 potential. The labels for the angles and bond lengths are in accord with the data in Table II. The dark lines represent covalent bonds between H and F atoms on the same molecule and the light double lines represent the hydrogen bonds.

simulated annealing procedure employed by Freeman, Doll, and Amar.[37] Starting with the system in the *cis* open chain geometry, we instantaneously heat the confined cluster to temperature T and propagate the system with Brownian dynamics for a fixed time period. We then instantaneously quench the system to zero degrees. The rate at which the system will escape the local potential barrier is proportional to the fraction of total trajectories whose final structure differs from the initial structure. Assuming Arrhenius behavior, a plot of the logarithm of the rate as a function of $1/T$ gives the activation barrier from the slope. Using this method we found the activation energy to be approximately 0.5 kcal mol^{-1}, or about 20% of the energy difference between the isomers depicted in Figs. 1 and 2. Further investigation of high energy isomers by *ab initio* methods is warranted.

To our knowledge, the only information on the HF tetramer is the structural and energetic properties of $(HF)_4$ calculated in a square planar configuration.[13,17] Our Brownian quench studies have found the lowest energy configuration for the tetramer to be the puckered ring shown in Fig. 4. Figure 4(a) shows the evident symmetry from a top view, and the puckering is seen in the side view shown in Fig. 4(b). We believe the puckering is favored energetically because the bond lengths and angles become very close to those seen in the dimer (see the caption to Fig. 4). Such puckering is not possible in the trimer where the angles and bond lengths

TABLE II. Structural parameters for the cyclic HF trimer.

	r_1[a]	r_2[a]	α
Liu *et al.*[b]	0.909	2.692	26.3°
Karpfen *et al.*[c]		2.73	27°
Present	0.929	2.760	20.2°

[a] Distances in angstroms.
[b] Reference 17.
[c] Reference 16.

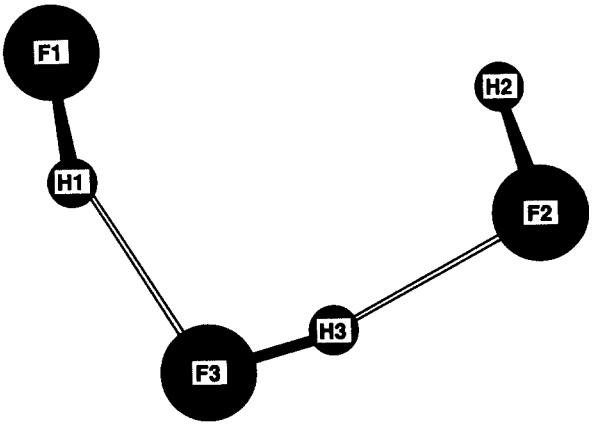

FIG. 3. The *cis* open chain structure for $(HF)_3$ obtained from the HF2 potential. The dark lines represent covalent bonds between H and F atoms on the same molecule and the light double lines represent the hydrogen bonds.

differ significantly from the dimer. We believe the relaxed puckered structure to be responsible for the stabilities of the tetramers which we will discuss in our thermodynamic calculations, below.

The two lowest energy structures we found for the hexamer are shown in Fig. 5. The lowest is reminiscent of the "boat" form of cyclohexane and the next lowest is the "chair" form. From our annealing studies, we found in excess of 100 local minima for the hexamer, although we made no extensive search to attempt to find all the local minima.

In Table III we give the potential energies $\hat{V}_n$ of the lowest energy isomer for cluster sizes $n = 2$ to 7. We also give the difference in energy between successive isomers, $\Delta\hat{V}_n = \hat{V}_n - \hat{V}_{n-1}$. The information in Table III will enable a structural analysis of the thermodynamic results to be discussed later.

IV. EVALUATION OF THE THERMODYNAMIC PROPERTIES

We performed calculations of the internal thermodynamic energy, entropy, and Gibbs free energy of the clusters

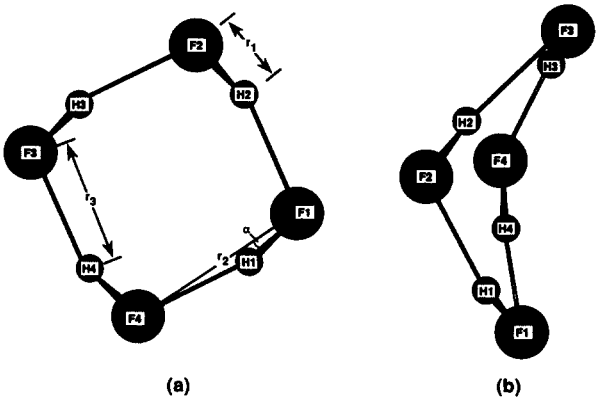

FIG. 4. The top (a) and side (b) views of cyclic $(HF)_4$. The dark lines represent covalent bonds between H and F atoms on the same molecule and the light double lines represent the hydrogen bonds. The bond lengths and angles, $r_1 = 0.932$ Å, $r_2 = 2.685$ Å, $r_3 = 1.783$ Å, and $\alpha = 11.8°$, are close to the values obtained in the dimer structure.

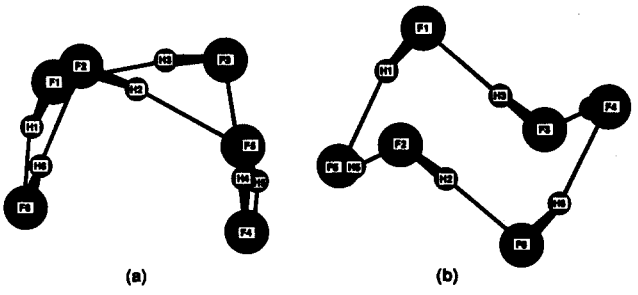

FIG. 5. The boat (a) and chair (b) forms of $(HF)_6$. The dark lines represent covalent bonds between H and F atoms on the same molecule and the light double lines represent the hydrogen bonds.

using standard Metropolis Monte Carlo methods.[39] Details of the Monte Carlo approach to computational statistical mechanics can be found in numerous other references,[40] and we make no effort to discuss the details here. As is well known, Monte Carlo methods are most suitable for the calculation of mechanical properties like the energy. For the nonmechanical properties like the entropy and the Gibbs free energy, a number of special techniques have been developed for cluster systems. In our calculations, we evaluated the Gibbs free energy by a modification of a method introduced by Mruzik, Abraham, Schreiber, and Pound[32] for calculations of the properties of ion–water clusters. The modifications of the original procedure were necessary owing to the intramolecular degrees of freedom included in this work and the continuous form of the constraining potential used. We sketch this approach below.

We wish to calculate the Gibbs free energy change for the process

$$(HF)_{n-1} + HF \rightarrow (HF)_n \tag{8}$$

in the approximation that all species obey the ideal gas law in a standard reference state of 1 atm pressure. From elementary statistical mechanics, the Gibbs free energy change ΔG_n associated with Eq. (8) can be written

$$\Delta G_n/RT = \ln\left[\frac{(q_n/L)}{(q_{n-1}/L)(q_1/L)}\right], \tag{9}$$

where L is Avogadro's number, and q_n is the molecular partition function for a cluster containing n molecules,

$$q_n = [1/(2n)!](2\pi m_H kT/h^2)^{3n/2}(2\pi m_F kT/h^2)^{3n/2} Z_n . \tag{10}$$

TABLE III. The total potential energy and potential energy difference of successive cluster sizes for the lowest energy isomer of each cluster size.

n	$\hat{V}_n$[a]	$\Delta\hat{V}_n$[a]
2	−6.40	−6.40
3	−16.97	−10.57
4	−27.75	−10.78
5	−35.00	−7.25
6	−43.93	−8.93
7	−52.50	−8.57

[a] Energies in kcal mol^{-1}.

In Eq. (10), Z_n is the standard configurational integral

$$Z_n = \int d^3r_{H_1}\, d^3r_{F_1}\, d^3r_{H_2} \cdots d^3r_{F_n} \times \exp[-\beta V_n(\mathbf{r}_{H_1},\ldots,\mathbf{r}_{F_n})] \tag{11}$$

$$\equiv \int d^{6n} \exp[-\beta V_n] , \tag{12}$$

where $\beta = 1/kT$ and V_n is the interaction potential for the cluster including the constraining potential. Using Eq. (10), Eq. (9) can be written

$$\Delta G_n/RT = -\ln L + \ln n - \ln[Z_n/(Z_{n-1}Z_1)] . \tag{13}$$

The ratio of configurational integrals appearing in Eq. (13) can be conveniently calculated by defining a scaled potential function $V(\lambda)$ given by

$$V(\lambda) = \Phi_{n-1} + \lambda V_{\text{int}} + V_c , \tag{14}$$

where Φ_{n-1} is the potential of a cluster consisting of $(n-1)$ molecules plus the Morse function on the nth molecule, V_c is the constraining potential for the full n molecule cluster, and V_{int} is the interaction potential between the nth molecule in the cluster and the remaining $(n-1)$ molecules. For example, for an HF trimer we write

$$V(\lambda) = \tilde{V}_1 + \tilde{V}_2 + \tilde{V}_3 + V_{12} + V_c + \lambda(V_{13} + V_{23}) , \tag{15}$$

where $\tilde{V}_i$ is the Morse function binding the hydrogen and fluorine atoms on molecule i, and V_{ij} is the interaction potential between molecules i and j. From Eq. (14) it is clear that

$$V(\lambda = 1) = V_n \tag{16}$$

and

$$V(\lambda = 0) = V_{n-1} + V_c + \tilde{V}_n . \tag{17}$$

We now define

$$Z(\lambda) = \int d^{6n}r \exp[-\beta V(\lambda)] . \tag{18}$$

From Eq. (18) we can write

$$Z(\lambda = 1) = Z_n \tag{19}$$

and

$$Z(\lambda = 0) = \int d^{6n}r \exp[-\beta(V_{n-1} + V_c + \tilde{V}_n)] \tag{20}$$

$$= \int d^{6(n-1)}r \exp[-\beta(V_{n-1} + V_{c_{n-1}})] \times \int d^6 r \exp[-\beta(\tilde{V}_n + V_{c_n})] . \tag{21}$$

In Eq. (21), $V_{c_{n-1}}$ and V_{c_n} are expressed as follows. We let $\mathbf{R}_{\text{c.m.},n-1}$ be the center of mass of the cluster consisting of $(n-1)$ molecules, and we let $\mathbf{R}_{\text{c.m.},1}$ be the center of mass of the tagged monomer. We define the center of mass for finite λ by

$$\mathbf{R}_{\text{c.m.}}(\lambda) = (\mathbf{R}_{\text{c.m.},n-1} + \lambda \mathbf{R}_{\text{c.m.},1})/(1+\lambda) . \tag{22}$$

Then $V_{c_{n-1}}$ is the constraining potential for the $(n-1)$ molecule cluster and

$$V_{c_n} = \{[\mathbf{R}_{HF} - \mathbf{R}_{c.m.}(\lambda = 0)]/R_c\}^{20}, \quad (23)$$

i.e., the constraining potential for the n molecule cluster defined with respect to the center of mass of the $(n-1)$ molecule cluster. Clearly,

$$\int d^{6(n-1)}r \exp[-\beta(V_{n-1} + V_{c_{n-1}})] = Z_{n-1}, \quad (24)$$

so that

$$Z(\lambda = 0) = Z_{n-1} \int d^6 r \exp[-\beta(\tilde{V}_n + V_{c_n})]. \quad (25)$$

If we transform the integral on the right-hand side of Eq. (25) to center of mass coordinates, we obtain

$$Z(\lambda = 0) = Z_{n-1} \int d^3 r \exp[-\beta \tilde{V}_n] \int d^3 R \times \exp[-\beta(R/R_c)^{20}] \quad (26)$$

$$\equiv \Omega_c Z_{n-1} \int d^3 r \exp[-\beta \tilde{V}_n]. \quad (27)$$

The second integral on the right-hand side of Eq. (26) can be viewed as an effective constraining volume Ω_c, which has been evaluated previously in argon cluster work,[25] and is given by

$$\Omega_c = (\pi/5)(kT)^{3/20} R_c^3 \Gamma(3/20), \quad (28)$$

where $\Gamma(x)$ is the gamma function.[41] It is easy to see that

$$Z_1 = \Omega \int d^3 r \exp[-\beta \tilde{V}_1], \quad (29)$$

where Ω is the molar volume. Then we can write

$$Z_n/(Z_{n-1}Z_1) = (\Omega_c/\Omega) Z(\lambda = 1)/Z(\lambda = 0), \quad (30)$$

so that

$$\Delta G_n/RT = -\ln(p/p_c) + \ln n - \ln[Z(\lambda = 1)/Z(\lambda = 0)], \quad (31)$$

where

$$p_c = RT/\Omega_c \quad (32)$$

and p is the pressure of the defined standard state (1 atm in our case). It is easy to show that

$$\ln[Z(\lambda = 1)/Z(\lambda = 0)] = \int_0^1 d\lambda \frac{\partial \ln Z(\lambda)}{\partial \lambda} \quad (33)$$

$$= -\beta \int_0^1 \langle V_{int} \rangle_\lambda d\lambda, \quad (34)$$

where the bracket in Eq. (34) implies a canonical average with respect to $V(\lambda)$, i.e.,

$$\langle V_{int} \rangle_\lambda = \int d^{6n} r \exp[-\beta V(\lambda)] V_{int} / \int d^{6n} r \times \exp[-\beta V(\lambda)]. \quad (35)$$

Equation (35) can be evaluated by the standard Metropolis Monte Carlo procedure.[39]

V. RESULTS

We performed calculations of the change in the internal energy, the Gibbs free energy, and the entropy of HF clusters associated with the processes expressed in Eq. (8). The internal energy was calculated using the standard Metropolis Monte Carlo algorithm.[39] The initial configuration for each cluster size was taken to be the lowest energy structure found in the Brownian dynamics simulated annealing calculations. Approximately one-million Monte Carlo moves were included during an initial warmup period followed by an additional one-million Monte Carlo moves during which data were accumulated. Moves were made sequentially for each atom in the cluster followed by periodic moves of the center of mass of each constituent molecule. The constraining radii were taken to be 5 Å for the dimer and 20 Å for the remaining clusters. Results of the energy calculations for 100 and 273 K are given in Table IV. The error bars listed in Table IV as well as in the tables which follow are at the single standard deviation level.

The Gibbs free energy change was calculated from Eqs. (34) and (35). In order to evaluate Eq. (34) a one-dimension integration over λ must be performed computationally. Since this integral is known to have numerical difficulties,[32,42] it is necessary to outline the approach used in this work. The key to an efficient evaluation of Eq. (34) is the application of Gauss quadrature techniques along with a judicious choice of the constraining radius. As observed in studies of argon clusters[31] and as we shall see in the current work on HF, the calculated free energies are insensitive to the value chosen for the constraining radius. We found the functional dependence of $\langle V_{int} \rangle_\lambda$ on λ to be quite sensitive to the choice of R_c. Since the calculated value of ΔG_n is roughly independent of R_c, the constraining radius can be chosen to facilitate numerical evaluation of the integration in Eq. (34). As an example, in Fig. 6 we plot $\langle V_{int} \rangle_\lambda$ for a dimer at 100 K as a function of λ for various values of R_c. The expression for $\langle V_{int} \rangle_\lambda$ was evaluated from Eq. (35) using standard Metropolis Monte Carlo methods.[39] The initial configuration was taken to be the structure which minimized $V(\lambda)$ as obtained from a Brownian quench study of the scaled potential function. As in the energy calculations, approximately one-million Monte Carlo moves were included in a warmup step followed by one-million Monte Carlo passes where data were accumulated. As seen in Fig. 6, $\langle V_{int} \rangle_\lambda$ becomes very sharply peaked for small λ. This same behavior has been noted in previous work on water cluster ions[32] and impuri-

TABLE IV. The change in the thermodynamic energy associated with the process given in Eq. (8) as a function of cluster size at 100 and 273 K.

n	ΔU_n (100 K)[a]	ΔU_n (273 K)[a]
2	-5.91 ± 0.02	-4.60 ± 0.05
3	-10.11 ± 0.02	-7.02 ± 0.2
4	-9.99 ± 0.02	-10.63 ± 0.4
5	-6.53 ± 0.06	-5.86 ± 0.5
6	-7.54 ± 0.18	-6.29 ± 0.5
7	-7.02 ± 0.36	-6.11 ± 0.5

[a] Energies in kcal mol^{-1}.

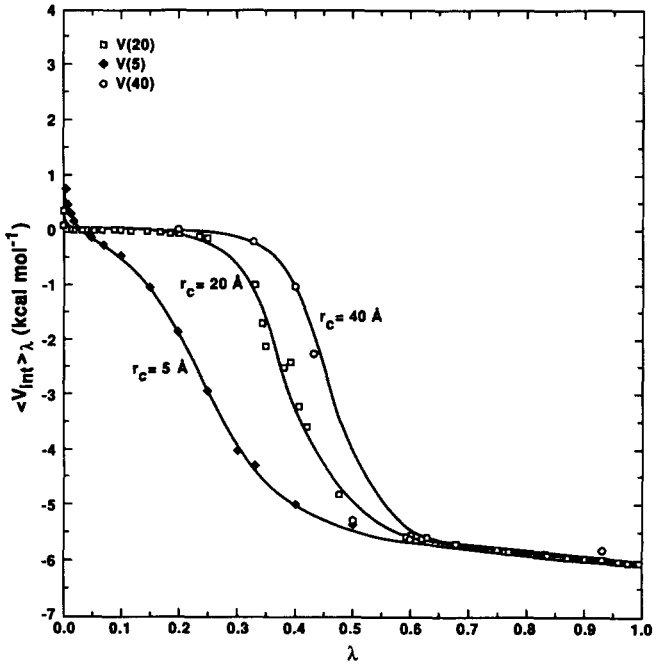

FIG. 6. $\langle V_{\rm int}\rangle_\lambda$ as a function of λ for $R_c = 5$ (closed diamonds), 20 (open squares), and 40 (circles). The smoother behavior of the functional dependence on λ for small R_c is evident from the figure.

ties in crystal lattices.[42] The sharp rise in $\langle V_{\rm int}\rangle_\lambda$ for small λ makes the numerical integration in Eq. (34) rather difficult. It is also clear from Fig. 6 that the region of small λ over which $\langle V_{\rm int}\rangle_\lambda$ changes rapidly is only a nominal fraction of the total range of λ values in the HF cluster system. Consequently, the small range can be expected to make little contribution to the total integral in the case of HF. Data to verify this unimportance of the contribution from the small λ region are given in Table V. In Table V we give contributions to the overall integration from the region from 0 to 0.02 and 0.02 to 1 separately as a function of the number of Gauss–Legendre quadrature points included n and the constraining radius R_c for a dimer at 100 K. The contribution from the region for $\lambda = 0$ to 0.02 is well within the statistical uncertainty of the calculation of the total integral. In the final column of Table V, we give the result of a numerical evaluation of the integral using Gauss–Legendre points appropriate for the interval [0,1]. In this last column, the special difficulties of the integrand for small λ are completely ignored. The differences between the results given in the last column and the sum of the preceding two columns are within the statistical uncertainties of the calculations. We found similar results in calculations performed at 273 K. From Fig. 6 it is clear that the functional behavior of the integrand on λ is smoother for small R_c than for large R_c. As we shall show in the next paragraph, the free energy calculated is very weakly dependent on R_c. Consequently, in the calculations, we chose small values of R_c to facilitate the convergence with respect to the number of Gauss–Legendre points.

TABLE V. The results of the one-dimensional λ integration as a function of the number of quadrature points n and the constraining radius R_c for a dimer at 100 K.

n	R_c[a]	$\int_0^{0.02}\langle V_{\rm int}\rangle_\lambda d\lambda$[b]	$\int_{0.02}^{1}\langle V_{\rm int}\rangle_\lambda d\lambda$[b]	$\int_0^1\langle V_{\rm int}\rangle_\lambda d\lambda$[b]
4	5	0.026 ± 0.005	-4.20 ± 0.02	-4.25 ± 0.02
4	20	0.0003 ± 0.0002	-3.38 ± 0.15	-3.21 ± 0.15
6	20	0.0004 ± 0.0002	-3.39 ± 0.15	-3.47 ± 0.15
8	20	0.0005 ± 0.0002	-3.40 ± 0.15	-3.48 ± 0.15
4	40	0.0004 ± 0.0002	-2.96 ± 0.15	-3.03 ± 0.15

[a] Distances in angstroms.
[b] Energies in kcal mol^{-1}.

TABLE VI. The Gibbs free energy change at 1 atm pressure and 100 K for the formation of $(HF)_2$ as a function of the number of quadrature points n and the constraining radius R_c.

R_c (Å)\n	4[a]	6[a]	8[a]
5	-3.51 ± 0.02	-3.41 ± 0.03	-3.43 ± 0.02
10	-3.48 ± 0.05		
15	-3.29 ± 0.05		
20	-3.20 ± 0.05	-3.46 ± 0.05	-3.47 ± 0.05
30	-3.24 ± 0.05		
40	-3.36 ± 0.10	-3.43 ± 0.15	-3.79 ± 0.16

[a] Energies in kcal mol^{-1}.

A measure of the sensitivity of the free energy to the number of quadrature points included in the evaluation of Eq. (34) and the constraining radius is given in Table VI. The calculations are for the dimer at 100 K. In Table VII we give the free energy change for the reaction of the dimer and monomer to form trimer at 100 K as a function of the number of quadrature points included in the evaluation of Eq. (34). In this case the constraining radius was taken to be 20 Å. We find six quadrature points to be adequate, and the calculated free energy change to be independent of the size of the constraining potential to within the precision of the calculation.

In Table VIII we list the calculated Gibbs free energy changes associated with Eq. (8) at 100 and 273 K. The constraining radii were taken to be 5 Å for the dimer, 8 Å for the trimer, 10 Å for the tetramer and the pentamer, and 12 Å for the hexamer and the heptamer. Six Gauss–Legendre quadrature points were used in the evaluation of Eq. (34). The cluster size listed corresponds to the right-hand side of Eq. (8). For all cluster sizes, the Gibbs free energy changes were calculated with approximately the same number of Monte Carlo points. We believe the marked increase in the variance

TABLE VII. The Gibbs free energy change for the reaction of HF with $(HF)_2$ at 1 atm pressure as a function of the number of quadrature points n at 100 K for a constraining radius of 20 Å.

n	ΔG_3[a]
4	-6.9 ± 0.1
6	-6.49 ± 0.11
8	-6.41 ± 0.10

[a] Energies in kcal mol^{-1}.

TABLE VIII. The Gibbs free energy change associated with Eq. (8) as a function of cluster size at 1 atm pressure.

	ΔG_n (100 K)[a]	ΔG_n (273 K)[a]
$(HF)_2$	-3.42 ± 0.02	$+0.99 \pm 0.14$
$(HF)_3$	-6.19 ± 0.10	-0.04 ± 0.09
$(HF)_4$	-6.84 ± 0.28	-1.23 ± 0.30
$(HF)_5$	-4.37 ± 0.20	-0.58 ± 0.40
$(HF)_6$	-5.31 ± 0.35	-0.15 ± 0.80
$(HF)_7$	-5.70 ± 0.40	$+0.09 \pm 0.70$

[a] Energies in kcal mol^{-1}.

with cluster size is a consequence of the increasing numbers of structures available to the aggregates as n increases. The entropy change for the growth process can be calculated from the usual expression

$$\Delta S = (\Delta H - \Delta G)/T \tag{36}$$

and the results of the entropy changes are given in Table IX.

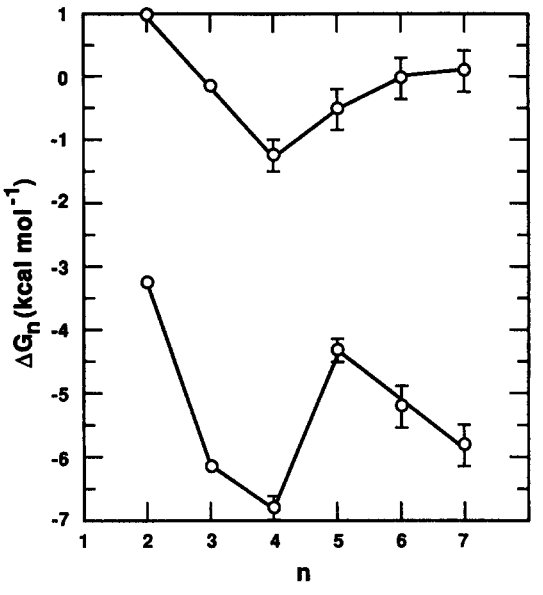

FIG. 7. ΔG_n as a function of n at a pressure of 1 atm. The free energy is expressed in kcal/mol. The upper graph is calculated at a temperature of 273 K and the lower graph at 100 K. Single standard deviation error bars are included for each point. The points are connected by straight lines for clarity. The minimum at $n = 4$ is clearly evident.

VI. DISCUSSION

In previous studies of the thermodynamic properties of argon clusters, magic numbers of extra stability were identified by minima in the Gibbs free energy as a function of cluster size.[26] To clarify the relative stabilities of hydrogen fluoride clusters, a graph of ΔG_n is given in Fig. 7. The lower curve represents ΔG_n at 100 K and the upper curve gives the calculated results at 273 K. At both temperatures, there is a well defined minimum at $n = 4$. The relative depth of the free energy function about the tetramer is evidently more pronounced at low temperatures, but the minimum is present under all conditions studied in this work.

An understanding of the extra stability associated with the tetramer can be obtained by examining the structures previously discussed in Sec. III. As mentioned, in forming the planar ring structure for the trimer, the hydrogen bond angles and lengths are significantly distorted from those observed in the dimer. Although two additional hydrogen bonds are formed in making the cyclic trimer, the energy gained can be expected to be diminished owing to the strains arising from the distortions. In contrast, the tetramer structure is puckered so that the bond lengths and angles which seem to be natural for the system (as determined by the dimer structure) can be secured. We can measure the effect of strain on the system by examining the energy of each cluster per hydrogen bond. The energy per hydrogen bond E_b is given in Table X at 0, 100, and 273 K. The structure at 0 K is assumed to be the lowest energy isomer, whereas at the higher temperatures, all structures contribute owing to the Boltzmann distribution. The decrease in E_b is evident for the trimer at all three temperatures. There is a dramatic increase in E_b for the tetramer. Indeed, for $(HF)_4$, the energy per hydrogen bond is greater than the dimer by 0.54 kcal mol^{-1} at 0 K. It is likely that the extra energy for the tetramer is a result of the additional favorable interactions possible when the ring puckers. The extra energy per hydrogen bond increases as the size of the rings increase, again providing evidence for the importance of the additional interactions when the structures are nonplanar.

The preceding discussion of stability is based on energetic arguments. In the previous studies of argon clusters,[26] it was found that entropic effects were relatively unimportant in determining relative stabilities. Similarly, the entropy function is relatively smooth in the case of HF clusters as can be seen in Table IX.

The temperatures chosen in this work are representative

TABLE IX. The entropy change associated with Eq. (8) as a function of cluster size and temperature at 1 atm pressure.

	ΔS_n (100 K)[a]	ΔS_n (273 K)[a]
$(HF)_2$	-27.0 ± 0.3	-22.5 ± 1.5
$(HF)_3$	-41.2 ± 1.0	-27.6 ± 2.0
$(HF)_4$	-35.5 ± 2.8	-36.4 ± 3.0
$(HF)_5$	-25.6 ± 2.1	-21.4 ± 3.5
$(HF)_6$	-25.3 ± 3.9	-24.5 ± 4.0
$(HF)_7$	-17.2 ± 5.4	-24.7 ± 4.3

[a] Entropies in cal mol^{-1} K^{-1}.

TABLE X. The energy per hydrogen bond as a function of cluster size and temperature.

	E_b (0 K)[a]	E_b (100 K)[a]	E_b (273 K)[a]
$(HF)_2$	-6.40	-5.71 ± 0.04	-4.05 ± 0.05
$(HF)_3$	-5.67	-5.24 ± 0.04	-3.61 ± 0.05
$(HF)_4$	-6.94	-6.45 ± 0.04	-5.29 ± 0.10
$(HF)_5$	-7.00	-6.49 ± 0.04	-5.35 ± 0.20
$(HF)_6$	-7.32	-6.70 ± 0.05	-5.46 ± 0.20
$(HF)_7$	-7.50	-6.74 ± 0.05	-5.52 ± 0.20

[a] Energies in kcal mol^{-1}.

of HF vapor in equilibrium with its solid (100 K) and liquid (273 K) phases. Physical hydrogen fluoride melts at 181 K and boils at 292 K. Of course the melting and boiling points associated with the HF2 potential are unknown. As in any numerical simulation, the extent to which the conclusions are an artifact of the chosen potential function must be questioned. The structures predicted by the HF2 potential for the dimer and trimer agree well with known information, and the structural features associated with the tetramer and hexamer are very intuitive. Confirmation of the tetramer and hexamer structures by careful *ab initio* calculations would be welcome. In spite of the inherent limitations in the HF2 potential, we feel it to be very likely that $(HF)_4$ is a very important species in physical hydrogen fluoride vapor.

In the current work, we have ignored quantum contributions to the internal motions. Such quantum effects may be of particular importance in this system, since the zero point motions can be expected to weaken the hydrogen bonds. Investigations of the importance of quantum contributions using Fourier path integral methods[34] are in progress.

ACKNOWLEDGMENTS

We would like to thank Sze Yang, Karen Peterson, Clair Cheer, and Ken Forcé for a number of very interesting discussions. Acknowledgment is made to the donors of the Petroleum Research Fund of the American Chemical Society for partial support of this work. This work was also supported in part by grants from Research Corporation, the University of Rhode Island Academic Computer Center, and the University of Rhode Island Engineering Computer Laboratory.

[1]D. F. Smith, J. Chem. Phys. **48**, 1429 (1968).
[2]T. R. Dyke, B. J. Howard, and W. Klemperer, J. Chem. Phys. **56**, 2442 (1972).
[3]M. F. Vernon, J. M. Lisy, D. J. Krajnovich, A. Tramer, H.-S. Kwok, Y. R. Shen, and Y. T. Lee, Faraday Discuss. Chem. Soc. **73**, 387 (1982).
[4]A. S. Pine and W. J. Lafferty, J. Chem. Phys. **78**, 2154 (1983).
[5]B. J. Howard, T. R. Dyke, and W. Klemperer, J. Chem. Phys. **81**, 5417 (1984).
[6]H. S. Gutowsky, C. Chuang, J. D. Keen, T. D. Klots, and T. Emilsson, J. Chem. Phys. **83**, 2070 (1985).
[7]A. S. Pine and B. J. Howard, J. Chem. Phys. **84**, 590 (1986).
[8]D. W. Michael and J. M. Lisy, J. Chem. Phys. **85**, 2528 (1986).
[9]P. V. Huong and M. Couzi, J. Chim. Phys. **66**, 1309 (1969).
[10]B. Desbat and P. V. Huong, J. Chem. Phys. **78**, 6377 (1983).
[11]J. Janzen and L. S. Bartell, J. Chem. Phys. **50**, 3611 (1969).
[12]F. A. Cotton and G. Wilkenson, *Advanced Inorganic Chemistry*, 5th ed. (Wiley, New York, 1988), Chap. 3.
[13]J. E. Del Bene and J. A. Pople, J. Chem. Phys. **55**, 2296 (1973).
[14]J. F. Gaw, Y. Yamaguchi, M. A. Vincent, and H. F. Schaefer III, J. Am. Chem. Soc. **106**, 3133 (1984).
[15]G. E. Scuseria and H. F. Schaefer III, Chem. Phys. **107**, 33 (1986).
[16]A. Karpfen, A. Beyer, and P. Schuster, Chem. Phys. Lett. **102**, 289 (1983).
[17]S.-Y. Liu, D. W. Michael, C. E. Dykstra, and J. M. Lisy, J. Chem. Phys. **84**, 5032 (1986).
[18]Z. Latajka and S. Scheiner, Chem. Phys. **122**, 413 (1988).
[19]W. L. Jorgensen and M. E. Cournoyer, J. Am. Chem. Soc. **100**, 4942 (1978).
[20]W. L. Jorgensen, J. Chem. Phys. **70**, 5888 (1979).
[21]M. L. Klein and I. R. McDonald, J. Chem. Phys. **71**, 298 (1979).
[22]A. E. Barton and B. J. Howard, Faraday Discuss. Chem. Soc. **73**, 45 (1982).
[23]G. C. Hancick, D. G. Truhlar, and C. E. Dykstra, J. Chem. Phys. **88**, 1786 (1988).
[24]W. L. Jorgensen, J. Am. Chem. Soc. **100**, 7824 (1978).
[25]D. L. Freeman and J. D. Doll, J. Chem. Phys. **82**, 462 (1985).
[26]D. L. Freeman and J. D. Doll, Adv. Chem. Phys. **70**, part 2, 139 (1988).
[27]I. A. Harris, R. S. Kidwell, and J. A. Northby, Phys. Rev. Lett. **53**, 2390 (1984).
[28]K. P. Huber and G. Herzberg, *Molecular Spectra and Molecular Structure. IV. Constants of Diatomic Molecules* (Van Nostrand Reinhold, New York, 1979).
[29]F. H. Stillinger, Isr. J. Chem. **14**, 130 (1975).
[30]F. H. Stillinger, J. Chem. Phys. **38**, 1486 (1963).
[31]J. K. Lee, J. A. Barker, and F. F. Abraham, J. Chem. Phys. **58**, 3166 (1973).
[32]M. R. Mruzki, F. F. Abraham, D. E. Schreiber, and G. M. Pound, J. Chem. Phys. **64**, 481 (1976).
[33]W. C. Swope, H. C. Andersen, P. H. Berens, and K. R. Wilson, J. Chem. Phys. **76**, 637 (1982).
[34]D. L. Freeman and J. D. Doll, J. Chem. Phys. **80**, 5709 (1984).
[35]F. H. Stillinger and T. A. Weber, Phys. Rev. A **28**, 2408 (1983).
[36]R. Biswas and D. R. Hamann, Phys. Rev. B **34**, 895 (1986).
[37]D. L. Freeman, J. D. Doll, and F. Amar (to be published).
[38]S. Chandrasekhar, Rev. Mod. Phys. **15**, 1 (1943).
[39]N. Metropolis, A. W. Rosenbluth, M. H. Rosenbluth, A. H. Teller, and E. Teller, J. Chem. Phys. **21**, 1087 (1953).
[40]J. P. Valleau and S. G. Whittington, in *Statistical Mechanics*, edited by B. J. Berne (Plenum, New York, 1977), p. 137.
[41]M. Abromowitz and I. A. Stegun, *Handbook of Mathematical Functions*, Natl. Bur. Stand. (U. S. GPO, Washington, D. C., 1964).
[42]D. R. Squire and W. G. Hoover, J. Chem. Phys. **50**, 701 (1969).

The Journal of Chemical Physics is copyrighted by the American Institute of Physics (AIP). Redistribution of journal material is subject to the AIP online journal license and/or AIP copyright. For more information, see http://ojps.aip.org/jcpo/jcpcr/jsp
Copyright of Journal of Chemical Physics is the property of American Institute of Physics and its content may not be copied or emailed to multiple sites or posted to a listserv without the copyright holder's express written permission. However, users may print, download, or email articles for individual use.

The Journal of Chemical Physics is copyrighted by the American Institute of Physics (AIP). Redistribution of journal material is subject to the AIP online journal license and/or AIP copyright. For more information, see http://ojps.aip.org/jcpo/jcpcr/jsp